# Comparison of the Josephson Voltage Standards of the NIST and the BIPM

**(part of the ongoing BIPM key comparison BIPM.EM-K10.b)**

S. Solve, R. Chayramy, and M. Stock
Bureau International des Poids et Mesures
F- 92312 Sèvres Cedex, France


Yi-hua Tang, and June E. Sims
Quantum Electrical Metrology Division
National Institute of Standards and Technology
100 Bureau Drive
Gaithersburg, MD 20899-8171, USA

# Comparison of the Josephson Voltage Standards
# of the NIST and the BIPM

## (part of the ongoing BIPM key comparison BIPM.EM-K10.b)

S. Solve and R. Chayramy, M. Stock
Bureau International des Poids et Mesures
F- 92312 Sèvres Cedex, France

Yi-hua Tang, and June E. Sims
Quantum Electrical Metrology Division
National Institute of Standards and Technology
100 Bureau Drive
Gaithersburg, MD 20899-8171, USA

**Abstract.** A comparison of the 10 V Josephson array voltage standard of the Bureau International des Poids et Mesures (BIPM) was made with that of the National Institute of Standards and Technology (NIST), USA, in March 2009. For this exercise, three different measurement methods were carried out: the two different options of the BIPM.EM-K10.b comparison protocol as well as the measurement protocol applied by NIST. The results of both participants are in very good agreement and the overall relative standard uncertainty is 9.5 parts in $10^{11}$.

## 1. Introduction

In the framework of CIPM-MRA key comparisons, the BIPM performed a direct Josephson voltage standard (JVS) comparison with that of the National Institute of Standards and Technology (NIST), in March 2009. The transportable BIPM JVS was shipped to NIST and the comparison was carried out on-site.

This comparison followed the technical protocol for BIPM.EM-K10.b comparisons and was carried out for both options of the protocol:

Option A is where the BIPM operates its measurement setup that includes an analog detector EM N1a to measure the voltage difference between both Josephson arrays. This option requires both Josephson Voltage Standards to be stable on an identified Shapiro steps during the time of the measurement acquisition.

Option B is where the participating laboratory operates its own measurement setup that usually includes a numeric detector.

This article describes the technical details of the experiments which were carried out to achieve the final result of the comparison.

## 2. Comparison equipment

### *2.1 The BIPM JVS*

The BIPM JVS used in this comparison is comprised of the cryoprobe, the microwave equipment and the bias source for the Hypres 10 V SIS array (S/N: 2548E-6). The Gunn diode frequency was stabilized using an EIP 578B counter, and an ETL/Advantest stabiliser. To visualize the array *I-V* characteristics, while keeping the array floating from ground, an optical isolation amplifier was placed between the array and the oscilloscope; during the measurements, the array was disconnected from this instrument. An HP 34401A digital voltmeter (DVM) was inserted between the array voltage bias leads to measure the voltage in order to verify the step stability. As reported below, we could however perform the measurement without monitoring the voltage across the BIPM JVS that is the BIPM JVS was stable enough to be confident with it for remaining on the selected step.

The series resistance of the measurement leads was less than 3 Ω in total (both measurement leads), and the value of the thermal electromotive forces (EMFs) due to both JVS was found to range between 390 nV and 450 nV (Cf. **Fig.** 1). The insulation resistance between the measurement leads was greater than $1 \times 10^{11}$ Ω (Cf. Appendix A).
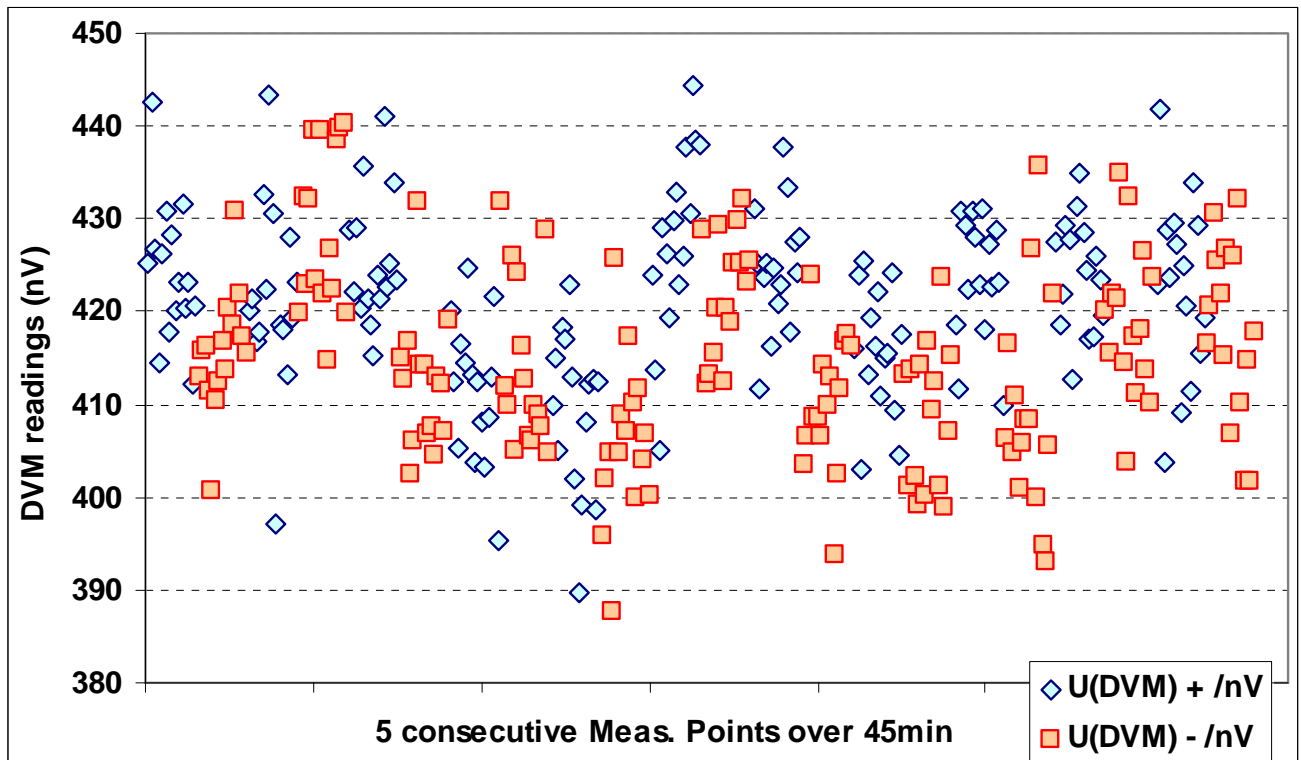
**Fig.**1. Example of the short term evolution of the thermal EMFs for the complete measurement loop during the comparison. *U*(DVM)+ is the reading of the detector once its positive polarity is on the NIST JVS side and *U*(DVM)- is the opposite situation. The readings are presented in terms of their absolute value.

### 2.2 The NIST JVS

The Compact Josephson voltage Standard (CJVS), constructed at NIST, uses a fixed microwave frequency of either 76.76 GHz or 76.84 GHz and integrates the microwave frequency assembly with the cryoprobe. The unique design of the microwave assembly eliminates the need of a frequency counter, thereby reducing the weight of the system. This makes the system compact and transportable. Fig.2 shows the microwave assembly. A 10 MHz quartz local oscillator is phase-locked to a 10 MHz frequency reference from a Global Positioning System (GPS) or Cesium clock. A quadrupler generates a 40 MHz frequency from the 10 MHz signal. Inside the cryoprobe, the 40 MHz signal is supplied as a reference to a Dielectric Resonance Oscillator (DRO) with an internal phase-lock loop (PLL) circuit. The DRO operates at 7.68 GHz. Its tenth harmonic 76.8 GHz is mixed with the 76.76 or 76.84 GHz Gunn Oscillator, creating a 40 MHz

intermediate frequency (IF). This 40 MHz IF output is appropriately amplified and mixed with the original 40 MHz quartz signal to provide a dc error signal. The error signal is provided to the Gunn tuner to generate a phase-locked stable microwave frequency at 76.76 GHz or 76.84 GHz for the Josephson array operation. The uncertainty of the fixed 76.76 GHz or 76.84 GHz frequency is determined by the 10 MHz frequency reference and is in the range of a few parts in $10^{12}$ or better. Commercial bias electronics and software developed at NIST control the measurement process.
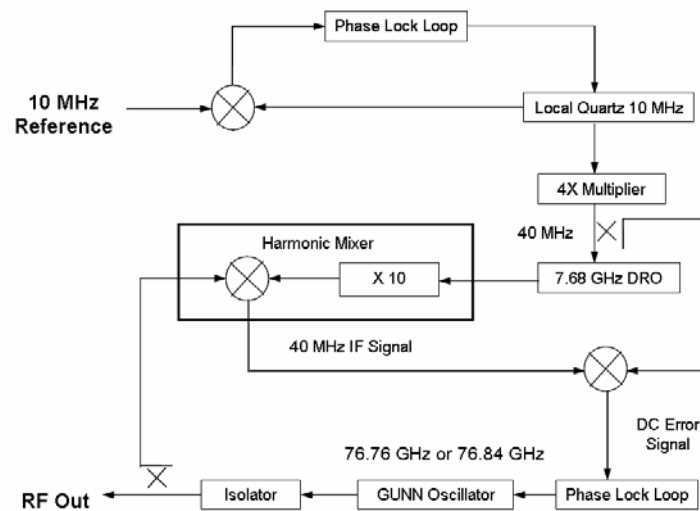
Fig.2. Block diagram of a 76.76 GHz source for Josephson array operation

Other details of the CJVS are as follows:
- Resistance of both precision measurement leads : 5.8 $\Omega$
- Leakage resistance between the precision measurement leads: 8.9 x $10^{10}$ $\Omega$
- Josephson junction array: Hypres 10 V SN2546E3
- Null detector: Agilent 34420A SN576912; range: 1 mV
- 10 V DVM: Agilent 34420A SN612213; range 10 V
- Bias source : VMetrix JVS1000
- Software : NISTVolt for Windows

## 3. Comparison procedures - Option B

In the option B, considered here, the BIPM only provides a reference voltage that has to be measured by the NIST using its Josephson standard with its own measuring device. The BIPM array is floating from ground.

## 3.1 Preliminary measurements

Within the week allotted to the comparison, different experiments were carried out in order to achieve the lowest voltage difference between the two JVS. The stability achieved on the two apparatuses, even when they were connected together was satisfactory enough that many measurement configurations could be tested. All the details of these test measurements are described in Appendix A.

Depending on the measurement configuration, the NIST CJVS array was either connected or disconnected from its bias source, which is itself referred to virtual ground (that is, not the  ground for the laboratory environment.

The BIPM bias source was operated on batteries during the step adjustment sequence, and was then disconnected from the array during the data acquisition process. The reference ground was connected to the NIST CJVS. The two arrays were connected in series-opposition via a dedicated NIST switch. In this comparison scheme (option "B"), the NIST CJVS was used to measure the BIPM array voltage as if it were a Zener voltage standard. During the comparison, only the biases of the two arrays were reversed (no mechanical switch reversal). This operation was done electronically on the NIST CJVS and manually on the BIPM JVS. The polarity reversal was typically completed within less than 1 s.

Once the BIPM equipment was set up and sufficiently stable conditions were found, the JVS was connected to the NIST measurement system and nine measurement points were acquired following the procedure applied by NIST.

The result was $(U_{\text{NIST}} - U_{\text{BIPM}}) / U_{\text{BIPM}} = + 1.5 \times 10^{-10}$.

The experimental standard deviation of the mean was 1.05 nV on 9 measurements points.

This comparison result shows the high reliability of the NIST Compact Josephson Voltage Standard (CJVS) and validates the CMCs of the laboratory. Following the preliminary measurements, a larger series of measurements was carried out where the measurement conditions were varied.

### 3.2 Description of the measurements (See also Appendix A)

**Operating setup for the first measurements**

The following is a brief description of the procedure used by NIST to obtain a single measurement of the voltage of the BIPM array. During the comparison, the BIPM current bias source was manually adjusted to select the same step after each polarity reversal. A fine adjustment on the voltage provided by the Digital to Analog Converter (DAC) of the CJVS bias current source was done through the software controlling the comparison. The NISTVolt program, written in Visual Basic$^{©}$ was also used to monitor the detector and record the data. The detector was a digital nanovoltmeter (HP34420A on the 1 mV range). Four sets of 15 readings of 10 powerline cycles each (NPLC=10) were taken, one set in the positive polarity of the bias of the two arrays, a second in the negative polarity, a third set in the positive polarity of the bias of the two arrays, and a fourth set in the negative polarity. The measurement followed the scheme: +, -, +, -. The recorded data were transferred to the computer through a GPIB interface. The complete series of measurements (+, -, +, -.) took about 8 minutes when there was no array instability. The readings were stored in an ASCII data file and the values attributed to the BIPM standard were also calculated by the software. The nanovoltmeter gain of the 1 mV range was measured before the comparison and the correction factor was applied to the results. In addition, a least-squares fit to the data was made after the acquisition to take into account any drift. After each polarity reversal we waited for 10 seconds before beginning data acquisition in order to avoid the larger effects of the discharge of the capacitors in the filters.

**Operating setup for the best measurements**

For all measurements, no significant changes to the routine NIST measurement were necessary. The measurement loop was arranged in such a way that both positive polarities of the arrays were connected together and the nanovoltmeter was placed in between the two negative polarities of the arrays. The "normal configuration" corresponds to the situation where the "High" of the nanovoltmeter was connected to the NIST array. The "reverse configuration" corresponds to the situation where the "Low" of the nanovoltmeter was connected to the NIST array. The 37 individual points used for the computation of the final result have been performed in the following configurations:

- Points #1 to #5: both arrays were biased at the frequency $f$ = 76.84 GHz. The measurements were performed in the "normal configuration".

-  Points #6 to #8: Those three points were performed in the "reverse configuration".

- Points #9 to #10: the biasing RF frequency of the BIPM standard was moved to $f$ = 76.850 GHz where the stability was better. Two points were carried out in the "reverse configuration".

- Points #11 to #15: Both RF biasing signals were moved to $f$ = 76.76 GHz and 5 points were performed in the "normal configuration".

- Points #16 to #25: 10 points were carried out in the "reverse configuration".

- Points #26 to #30: Those 5 points were performed in the "normal configuration".

7 Points were performed on 03/24/2009:

The grounding configuration of the measurement loop was modified the day before (Cf. Appendix A) and an option B protocol was followed for seven more measurements:

- Point #31: 1 point in the "normal configuration" after which some stability problems were encountered on the BIPM array. The origin was found on a probable malfunction of the Gunn diode.

- Points #32 to #37: The BIPM RF source was changed to another one for which the frequency was locked to $f$ = 74.549 570 GHz. For those points, the DVM monitoring the voltage across the BIPM array was removed. The measurements were carried out in the "normal configuration".

The differences between the values measured by the NIST CJVS and the theoretical value of the BIPM array voltage during the comparison are plotted on Fig. 3. A histogram of all 37 data points is shown is Fig. 4.
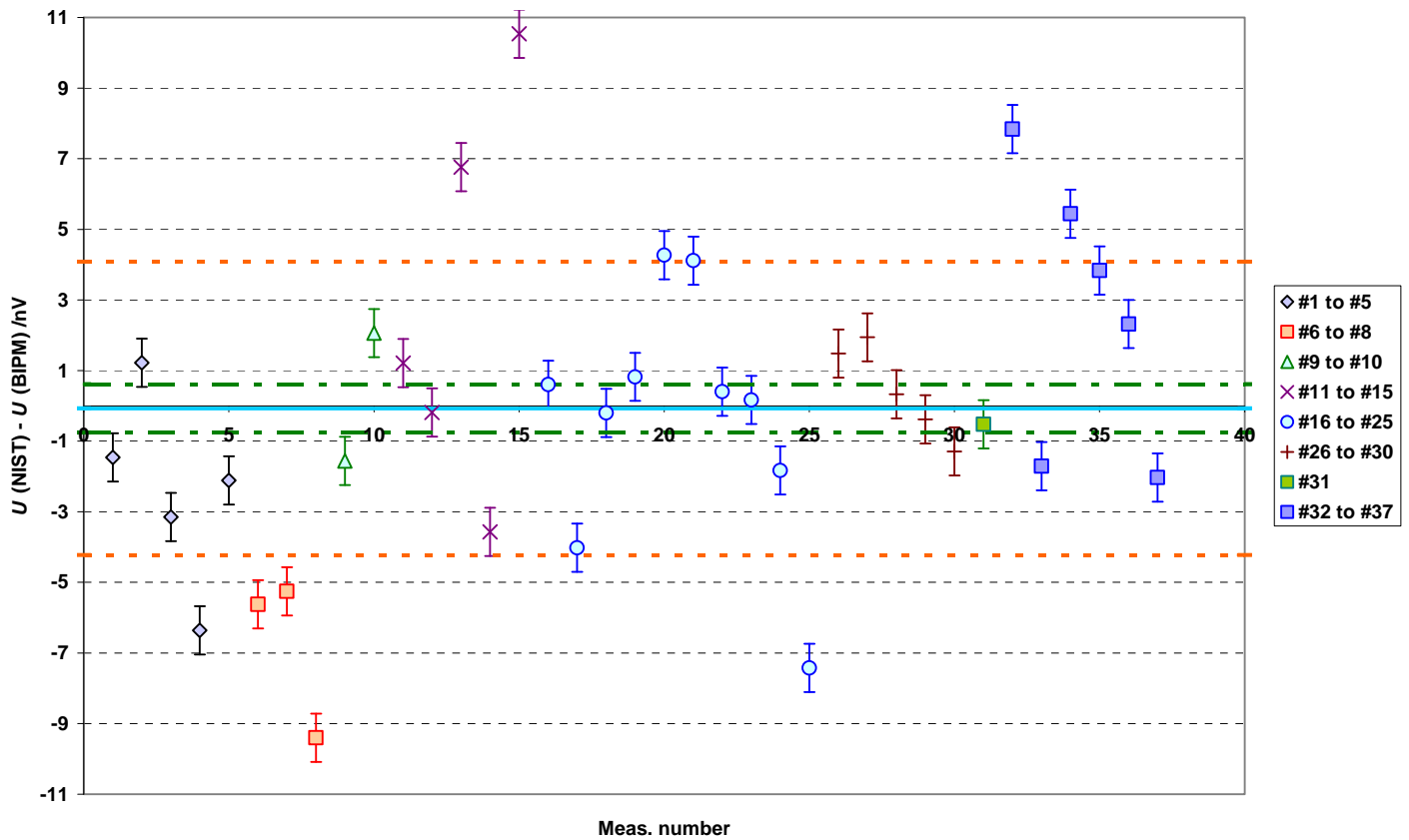
**Fig.** 3. Differences between the measured values and the theoretical value of the BIPM array voltage. The solid line represents the mean value, the dashed lines (– – –) represent the experimental standard deviation, and dotted-dashed lines (– —— –) are the experimental standard deviation of the mean assuming that all 37 points belong to the same statistical population and that there is no significant correlation between measurement values*. The error bars reflect the Type A uncertainty.
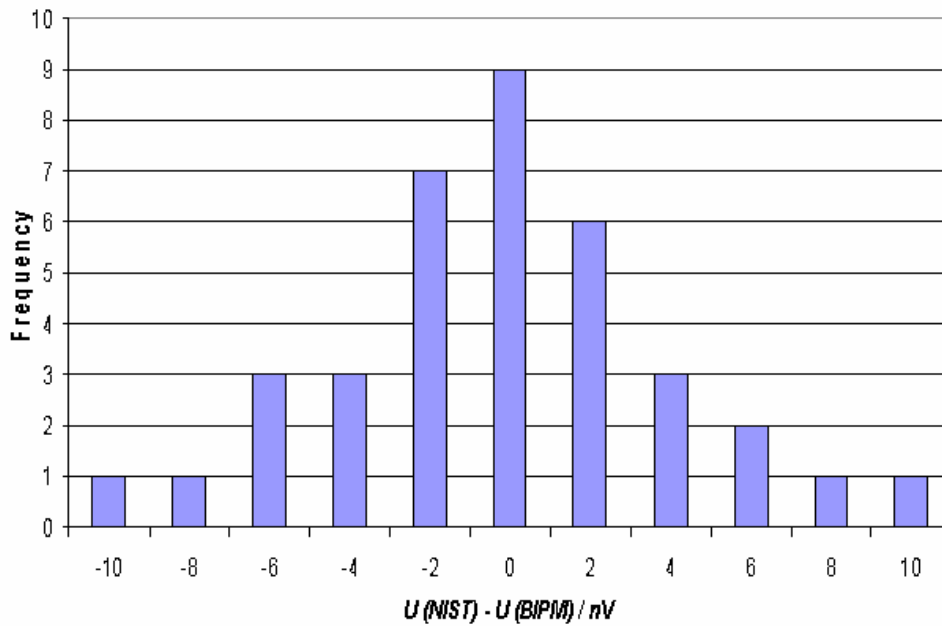
**Fig**. 4. The histogram of the JVS comparison using option B protocol.

* This assumption is supported by the estimated Birge ratio. We have calculated the standard deviation based on internal consistency for the 7 series of measurements (also called *a priori* uncertainty) which is given by: $\sigma_I^{-1} = \sum_j w_j$ where $w_j = \sigma_i^{-1}$ is the weight of the $j^{\text{th}}$ series, estimated by the reciprocal of the series' sample variance . This result was compared to the standard deviation based on external consistency (also called *a posteriori* uncertainty) calculated from $\sigma_E = \left[ \sum_j w_j \times (x_j - m_w)^2 \right] / \left[ (N-1) \sum_j w_j \right]$, where $N$ is the total number of series of measurements and $m_w$ is the weighted mean [1]. The Birge ratio is then given by $R_B = \sigma_E / \sigma_I$ and is equal to one if the consistency is perfect. In our case, $R_B$ = 1.24 ($\sigma_E$ = 1.124 nV and $\sigma_I$ =.0.904 nV). This result infers that the series of measurement values belong to the same statistical population and that no experimental parameter had a major influence on the day-to-day reproducibility.

### 3.3 Uncertainties and results

The sources of Type B uncertainty (Table 1) are: the frequency accuracy of the Gunn diodes, the leakage currents, and the detector gain and linearity. Most of the effects of detector gain and frequency stability are already contained in the Type A uncertainty. As both array polarities were reversed during the measurements, the effect of the residual thermal EMFs (i.e., non-linear drift) and electromagnetic interferences are also already contained in the Type A uncertainty of the measurements. Uncertainty components related to RF power rectification and sloped Shapiro

voltage steps are considered negligible as no such physical effect was observed. This was tested by fixing the bias current on a voltage step at several values above and below the step center and observing any possible voltage variations. None were observed.

| | Type | Uncertainty / nV | |
| --- | --- | --- | --- |
| | | BIPM | NIST |
| Frequency offset | B | 0.02[1] | 0.10 |
| Leakage resistance [2] | B | 0.30 | 0.65 |
| Detector [3] | B | | 0.58 |
| Total (RSS) | B | 0.30 | 0.88 |

**Table 1.** Estimated Type B standard uncertainty components.

([1]) As both systems are referred to the same 10 MHz frequency reference, the accuracy of the frequency sources is fixed by the 10 MHz reference thus only a Type B uncertainty from the frequency measured by the EIP is included [2]. The frequency reference used for the comparison is a high stability OCXO oscillator disciplined to Global Positioning System (GPS) signal. The Allen deviation of the oscillator is better than $1 \times 10^{-11}$ for averaging times ranging from 10 s to 1000 s [3]. The CJVS uses a fixed frequency and does not have a frequency counter. The uncertainty contribution from the frequency to the voltage measurement using NIST CJVS is therefore proportional to the Allen deviation during the voltage measurement which usually took around 500 s.

([2]) A detailed description is given in Appendix A.

([3]) A large part of the detector uncertainty is already contained in the Type A uncertainty of the measurements. This component only expresses the effect of the uncertainty of the detector non-linearity correction. The uncertainty due to DVM gain and linearity errors was estimated by multiplying the measured DVM gain uncertainty by the values of the Mean Polarized Null Voltage (MPNV) [3] that were made in the 37 comparison points. The relevant parameter for computing uncertainty due to DVM gain and linearity error is the mean of all of the values P(Set) x VDVM(Set) where P(Set) is the polarity of the measurement and VDVM is one of the i = 1 to 15 null voltage

measurements in each of the 4 sets using NISTVolt protocol. The average of all 37 MPNV made with option B was -84 µV and the DVM gain error was measured against NIST programmable JVS as -6.9 parts in $10^6$, resulting the Type B uncertainty component due to the DVM gain and linearity error as 0.58 nV.

The standard deviation of the mean of the 37 measurements was taken as Type A uncertainty and is equal to 0.68 nV.

The result using Option B, expressed as the relative difference between the values that would be attributed to the 10 V Josephson array standard by NIST ($U_{NIST}$) and its theoretical value ($U_{BIPM}$) is:

$$(U_{NIST} - U_{BIPM}) / U_{BIPM} = -7.4 \times 10^{-12} \quad \text{and} \quad u_c / U_{BIPM} = 1.2 \times 10^{-10}$$

where $u_c$ is the combined standard uncertainty.

## 4. Comparison procedures – Option A

As mentioned in the first paragraph, we observed very favorable experimental conditions so that an option A comparison was carried out.

### 4.1 Description of the measurements (also See Appendix A)

In the option A scheme, the BIPM uses its equipment to measure the voltage provided by the participant's JVS. The BIPM equipment consists of an EM model N1a analog nanovoltmeter (operated on its 3 µV range) whose output is connected, via an optically-coupled isolation amplifier, to a pen recorder and a digital voltmeter (DVM) HP34401A which is computer controlled via an IEEE bus.

The controling computer is used to monitor measurements, acquire data and calculate results. A low thermal electromotive force (EMF) switch which includes a voltage divider is used for critical switching, such as polarity reversal of the detector input and connection of both arrays in series opposition. The sensitivity switch is used to prevent the detector from overloading if both systems are not on their respective selected steps.

Once the NIST standard is connected to the BIPM measurement system, measurement points are acquired according to the following procedure:

1- Positive array polarity and reverse position of the detector;
2- Data acquisition;
3- Positive array polarity and normal position of the detector;

4- Data acquisition;

5- Negative array polarity and reverse position of the detector;

6- Data acquisition;

7- Negative array polarity and normal position of the detector;

8- Data acquisition;

9- Negative array polarity and reverse position of the detector;

10- Data acquisition

11- Negative array polarity and normal position of the detector;

12- Data acquisition;

13- Positive array polarity and reverse position of the detector;

14- Data acquisition;

15- Positive array polarity and normal position of the detector;

16- Data acquisition;

The reversal of the detector polarity is done to cancel out any detector offset error and thermo-electromotive forces.

Each "data acquisition" step consists of 10 preliminary measurements immediately followed by 30 other measurement. Each of these 30 measurements should not differ from the mean of the preliminary measurements by more than twice their standard deviation, otherwise the data are rejected and the acquisition is restarted. The "data acquisition" sequence lasts 25 s and is basically the time period during which both arrays are to stay on the selected step. The total measurement time (including polarity reversals and data acquisition) is approximately 5 minutes. We measured a total of twenty-two points between the 23$^{rd}$ of March and the 24$^{th}$ of March.

<u>11 Points were performed on 03/23/2009</u>:

The BIPM RF source was adjusted to the frequency $f$ = 76.764 880 GHz leading to a theoretical voltage difference value of ($U_{NIST} - U_{BIPM}$) = 0.76658 µV. These parameters are compatible with the 3 µV range of the N1a.

<u>11 Points were performed on 03/24/2009</u>:

In this series, the BIPM RF source was adjusted to the frequency $f$ = 74.549 480 GHz leading to a theoretical voltage difference value of ($U_{NIST} - U_{BIPM}$) = 0.18544 µV as the NIST CJVS was still operated at a frequency of 76.76 GHz.

The differences between the values measured by the BIPM and the theoretical value of the NIST array voltage during the option A comparison are plotted in Fig. 5.
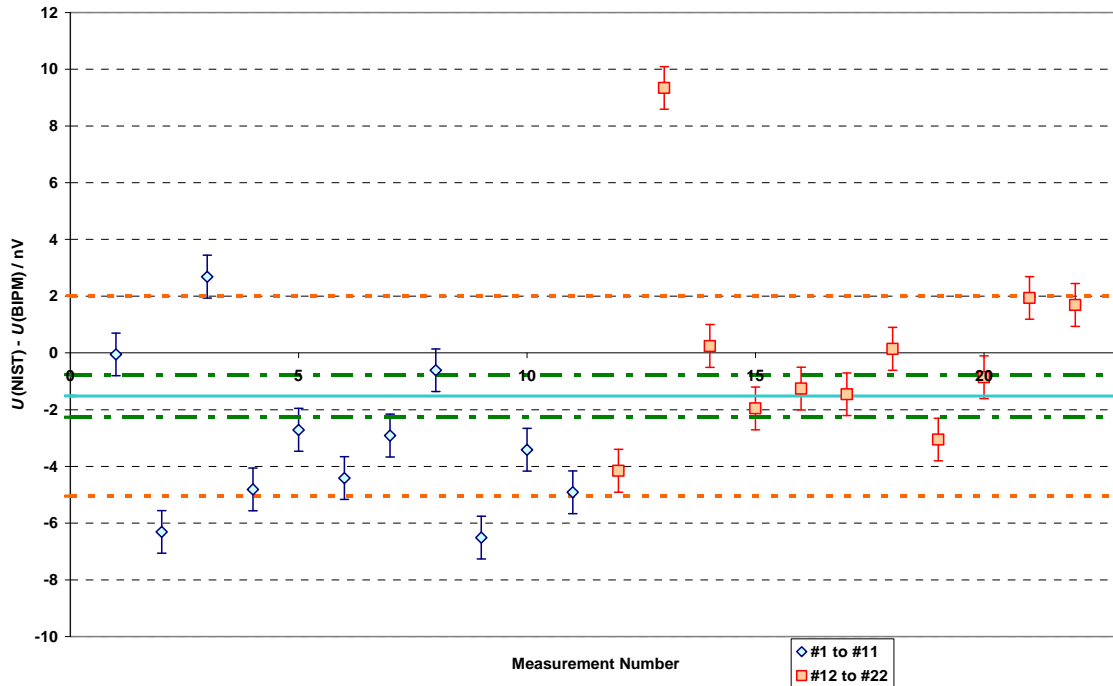


**Fig.** 5. Differences between the measured values and the theoretical value of the NIST array voltage (option A). The solid line represents the mean value, the dashed lines (– – –) represent the experimental standard deviation, and dotted-dashed lines (– - – - –) are the experimental standard deviation of the mean. The error bars reflect the Type A uncertainty.

## 4.2 Uncertainties and results

The BIPM uncertainty components, type and relative contribution are listed in **Table 2**:

| Uncertainty component | Type | Contribution / nV |
|:---:|:---:|:---:|
| Frequency [1] | B | 0.02 |
| Leakage resistance of the meas. leads [2] | B | 0.30 |
| Detector Calibration [3] | B | 0.25 |
| **Total RSS** | | **0.39** |

**Table 2.** Uncertainty components ($k$ = 1) for the voltage difference measurement with the BIPM equipment at 10 V (Option A).

([1]) As both systems are referred to the same 10 MHz frequency reference and most of the effects of the frequency stability are already contained in the Type A uncertainty, only a Type B uncertainty for the systematic errors of the EIP frequency measurement is included [2].

([2]) A detailed description is given in appendix A.

([3]) The BIPM "detector" is corrected for its gain. The calibration factors are calculated by the software before running the comparison. The calibration is based on the modification of the RF frequency biasing the array to obtain a full scale deviation (both in the positive and negative deflection). The readings of the N1a are compared to the corresponding theoretical voltage deflection given by the JVS.

The NIST uncertainty components, type and relative contribution are listed in **Table 3**:

| Uncertainty component | Type | Contribution / nV |
|---|---|---|
| Frequency [1] | B | 0.10 |
| Leakage resistance of the meas. leads [2] | B | 0.65 |
| Total RSS | | **0.66** |

**Table 3.** Uncertainty components ($k = 1$) for the voltage difference measurement with the NIST measurement setup (Option A).

([1]) Refer to Table 1 for the frequency uncertainty due to NIST CJVS.

([2]) The leakage resistance of measurement leads was measured during the comparison (Cf. Appendix A)

$R_L$ (NIST) = $8.9 \times 10^{10}$ $\Omega$. A detailed description is given in appendix A.

The standard deviation of the mean of the 22 measurement points is considered as the Type A uncertainty and is equal to 0.75 nV as we assume that the results are uncorrelated.

The result using Option A, expressed as the relative difference between the values that would be attributed to the NIST 10 V Josephson array standard by the BIPM ($U_{BIPM}$) and its theoretical value ($U_{NIST}$) is:

$$(U_{NIST} - U_{BIPM}) / U_{BIPM} = -1.53 \times 10^{-10} \quad \text{and} \quad u_c / U_{BIPM} = 1.1 \times 10^{-10}$$

where $u_c$ is the combined standard uncertainty.

## 5. Automatic measurements

### 5.1 Description of the measurements

Comparisons between the two JVS were also carried out in an automatic manner following the NIST-NRC protocol [5]. For this particular scheme, both JVS are biased with a common bias current source (NIST CJVS biasing source) and once both arrays are biased to the same voltage within a few steps, the acquisition is run following the measurement sequence described in §3.2 .

The purpose of a direct JVS comparison is to measure the real difference, $\delta$, of two JVS voltages from the theoretical value $V_d$.

$$V_d - V_m / (1 + E_g) = V_o + mt + V_n + \delta \qquad (2)$$

where $V_o + mt$ represents an offset voltage with a fixed and a linearly drifting component. The offset voltage is assumed to include both the voltmeter offset and thermal emf's in the measurement loop. $V_n$ is the random time dependent noise in the meter readings and any other unaccounted for effects such as DVM nonlinearity. $E_g$ is the gain error of the voltmeter. $\delta$ is the amount by which the measured voltage between the two standards differs from its theoretical value. Contributions to $\delta$ are

1. A discrepancy between $f_1$ or $f_2$ used in the equation and the actual frequencies applied to the Josephson arrays.
2. Leakage current $I_L$ that results in a voltage drop across the resistance of the measurement loop.
3. Uncorrected thermal offset and drift.
4. Any additional unknown effects.

Solving Eq. 2 for $\delta$ gives

$$\delta = V_d - V_m / (1+E_g) - V_o - mt - V_n \qquad (3)$$

The unknowns in this equation are $V_o$, $m$ and $\delta$. They can be estimated by making sets of measurements with two or more polarity reversals. Rather than using a reversing switch, the polarity of each array is reversed by changing the array bias to reverse the signs of $N_1$ and $N_2$ but not the magnitude. The data set is an array $V_d(i)$, $V_m(i)$, $t(i)$, and $P(i)$ for i = 1 to $N$ where $V_d(i)$ is the $i^{th}$ theoretical difference in array voltages, $V_m(i)$ is the $i^{th}$ meter reading, $t(i)$ is the time of the $i^{th}$ reading, $P(i)$ is the polarity of $V_{a1}$ and $V_{a2}$ for the $i^{th}$ reading, and $N$ is the total number of readings. Eq. 3 is a model for the data set. Best estimates for $V_o$ and $m$ and $\delta$ are computed using a 3 parameter fit that minimizes the RSS sum of the residuals $R(i)$ to the model of Eq. 3 where:

$$R(i) = V_d(i) - V_m(i) / (1+E_g) - V_o - mt(i) - \delta \qquad (4)$$

Simultaneous biasing of both arrays is achieved by insertion of a shorting switch in parallel with the nanovoltmeter. Fig. 6 shows the setup using the NIST CJVS to measure the BIPM JVS. With the nanovoltmeter shorted, the CJVS bias system biases both the CJVS array and the BIPM array to the same nominal voltage. Once both arrays reach the nominal voltage with the difference of the two arrays within 1 mV, the CJVS bias source is gradually disconnected from the two arrays via an optoisolator. The gradually increasing impedance of the optoisolator greatly reduces step jumps in both arrays when the bias is disconnected from the arrays. Opening the nanovoltmeter switch

usually resulted in a jump between the two arrays of one or two steps. An automatic switch controlled by the NISTVolt software was implemented in this comparison to improve the efficiency of the process. Note that the nanovoltmeter switch has no thermal EMF measurement contributions since it is an open circuit and not in the potential measurement loop.
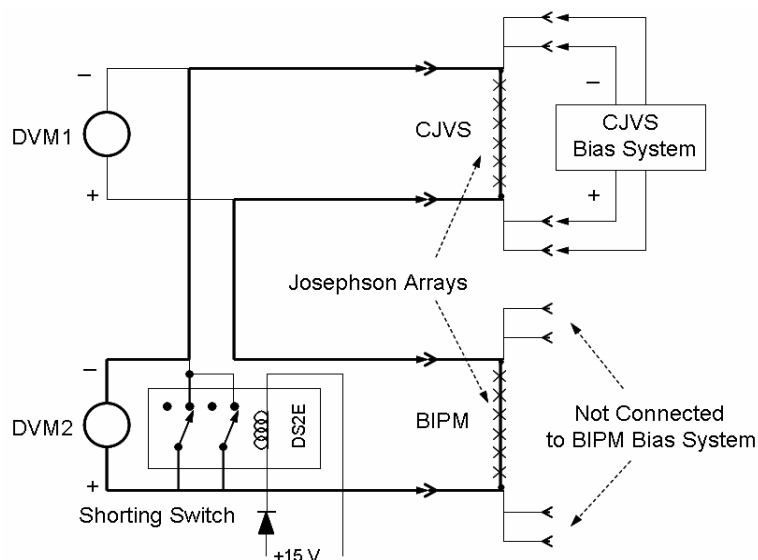


**Fig.** 6. The setup using the NIST CJVS to bias both the NIST CJVS array and the BIPM array. A shorting switch (a latching relay DS2E) for the DVM2 controlled by the NISTVolt software makes the automatic process possible.

As an example Fig.7 and Fig.8 show the results of an automatic run from 18:00 on March 21 to 8:20 on March 22 and the histogram of the measured voltage differences. A total of 218 points were made during 14.5 h. The drift in the difference between the CJVS and BIPM arrays over a long term might be related to the dewar pressure (Cf §6. Discussion). The mean difference $U$(NIST) – $U$(BIPM) between the measured difference and the theoretical difference of the two arrays is -0.70 nV.
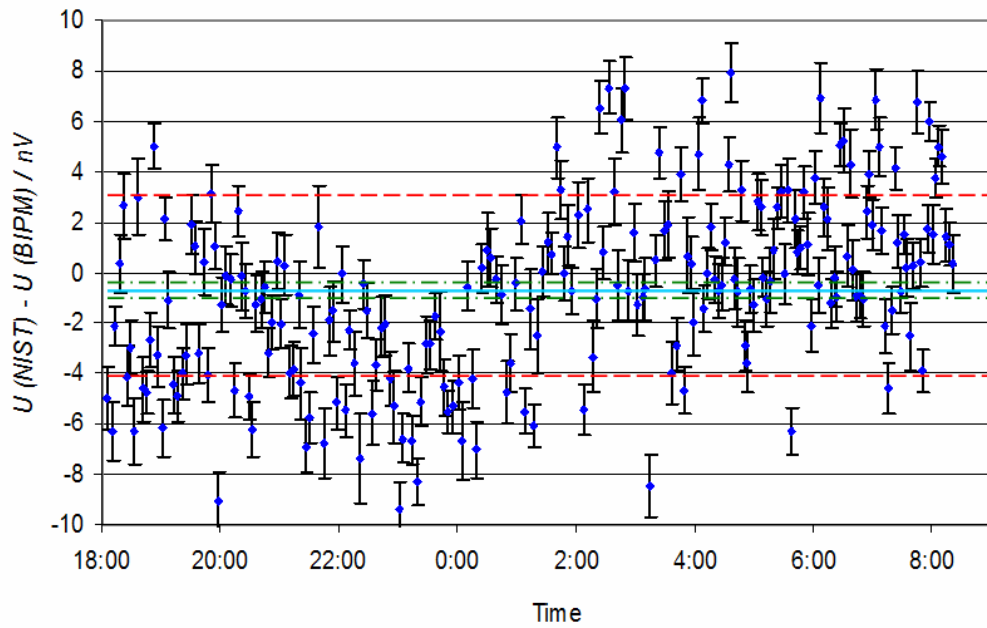
**Fig.** 7. Differences between the measured value and the theoretical value of NIST - BIPM at the nominal voltage of 9.997V made on March 21, 2009 using the NISTVolt automatic measurement protocol. The error bars show the Type A uncertainty of each measurement only. The solid line represents the mean value, the dashed lines (– – –) represent the experimental standard deviation and dotted-dashed lines (– —— –) are the experimental standard deviation of the mean.
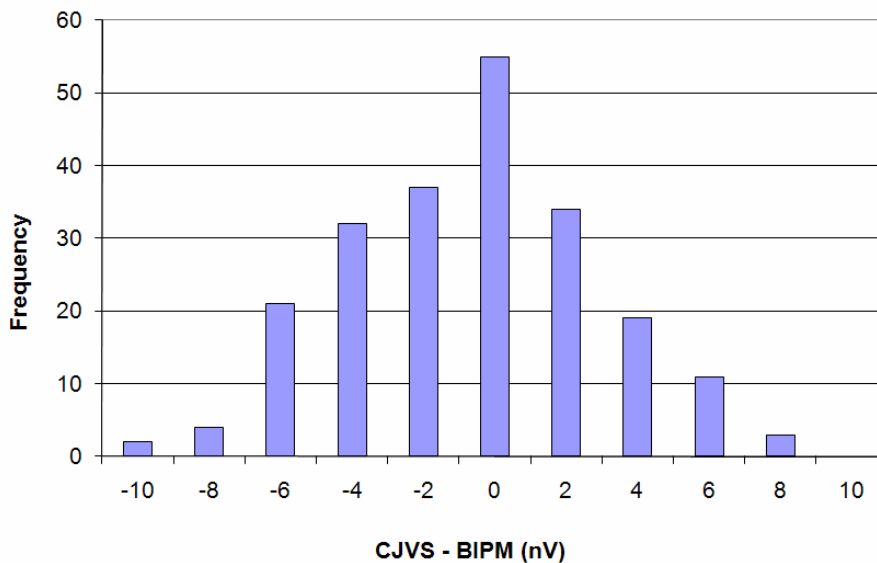
**Fig**. 8. Histogram of the automatic run of the JVS comparison on March 21, 2009 using the NIST protocol.

## 5.2 Impact of 1/f noise floor of DVM to Type A uncertainty

Throughout the course of the automatic measurements of the voltage differences between the two arrays, 31 measurements of the laboratory atmospheric pressure, $p$, were recorded. A correlation between the results of the voltage difference measurements and $p$ was observed. A linear least-squares fit yields a pressure coefficient of the voltage difference of -2.92 nV/hPa. This correlation is believed to originate from the effect of $p$ on the opening of a differential pressure relief valve meant to prevent overpressure in the helium Dewars. Changes in atmospheric pressure result in changes of pressure in the Dewar(s) which, in turn, produce small changes in the thermal electromotive forces (emf) in the precision voltage measurement leads.

Because the pressure measurements were made less often and at different times than the voltage measurements, a cubic spline method was used to interpolate an estimate of the pressure at the time of each voltage measurement. A correction of the voltage was made using the mean measured pressure as the reference value.
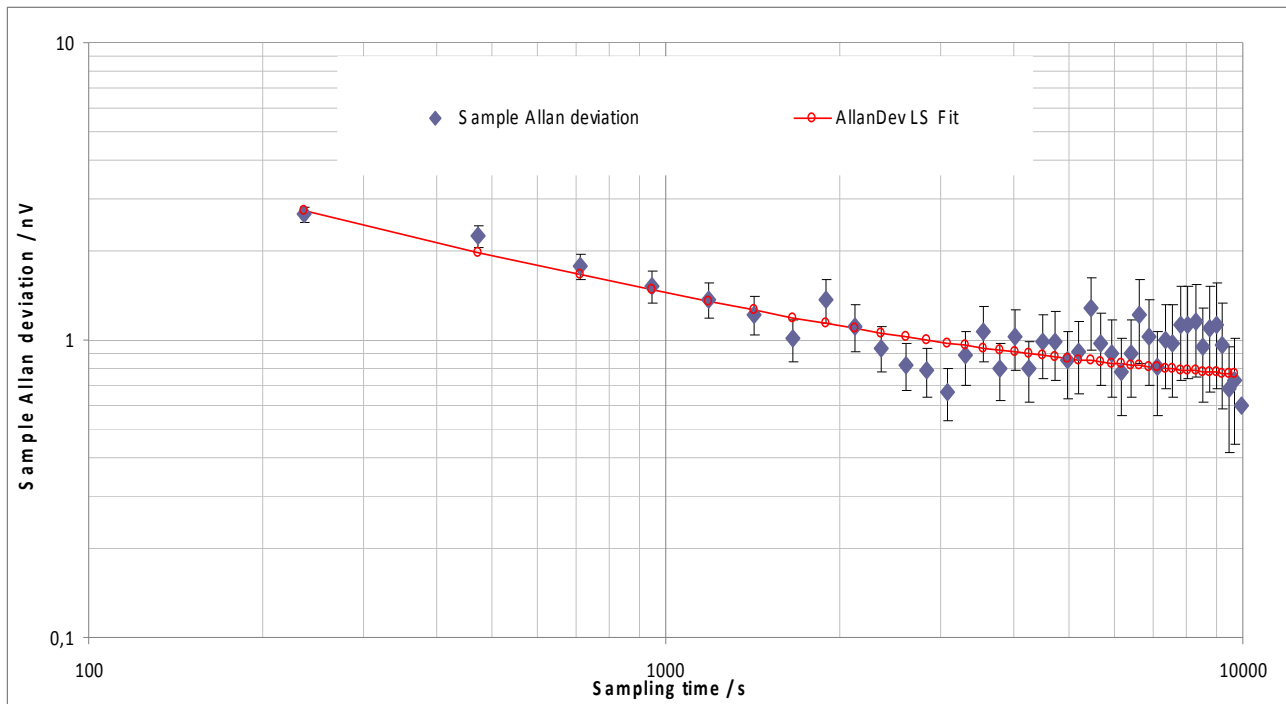
Fig. 9: (a) Sample Allan deviation estimated from the voltage differences in Fig. 7, between the two JVS; the bars represent $1\sigma$ confidence intervals. (b) Allan deviation for a model of mixed white and $1/f$ noise with parameters estimated from a weighted linear least-squares fit of the sample Allan variance.

The number of values of the voltage difference is great enough to carry out time series analyses of the results which, in turn, are used to check for (auto) correlations between measurement values. These analyses require that the interval between successive voltage measurements be constant, which is not the case. To adjust the measured voltage values to the estimated values which would have been observed had the time intervals been constant, another cubic spline interpolation was carried out. In this adjustment it is assumed that the time interval between successive measurements is equal to the average time interval. To account for correlations among successive values of the voltage difference between the two arrays, the sample Allan deviation was estimated from the voltage values interpolated to equal time intervals. This is plotted in Fig. 9 (a). The plot suggests that the estimated Allan variance, *Avar*, can be modeled as a mixture of white noise and $1/f$ noise of the form $Avar(\tau) = h_0/2\,\tau^{-1} + b$, where $\tau$ is the sampling time and $h_0$ and $b$ are constants related to the spectral density. The same form of the Allan variance was found in the analysis of voltage values measured with an HP 34420A with a short circuit at the input [5], Figure 1.

A weighted linear least-squares fit of *Avar* as a function of $\tau^{-1}$ results in an estimated value of $h_0/2$ of 1560 $nV^2$/Hz and of $b$ of 0.466 $nV^2$. The resulting Allan deviation is plotted in Fig.9 (b) as a

curved line. Although the total measurement time was 0.587 days (50 700 s), the uncertainty of the estimated Allan variance is such that credible estimates can be obtained for measurement times up to 1/4 of the total measurement time and so the Allan deviation of the measured values of the voltage differences is estimated to be $[(1650 \text{ nV}^2/\text{Hz})/12\ 700 \text{ s} + 0.422 \text{ nV}^2]^{1/2} = 0.75$ nV. This is taken as the type A standard uncertainty of the automatic measurements. The combined standard uncertainty of the automatic run was therefore calculated to be 1.14 nV. A detailed version of this analysis will be given in a later report.

### 5.3 Uncertainties and results

The uncertainty analysis is similar to that of the Option B. The sources of Type B uncertainty (Table 4) due to the frequency stability of the Gunn diodes and the leakage currents were identical to those for Option B, The Type B component due to the detector gain and linearity was estimated in the same way as in the Option B. The average of all 218 MPNV made with option B was -68 $\mu$V and the DVM gain uncertainty was measured against NIST programmable JVS as -6.9 parts in $10^6$, resulting the Type B uncertainty component due to the DVM gain and linearity error as 0.47 nV.

| | Type | Uncertainty / nV | |
| --- | --- | --- | --- |
| | | BIPM | NIST |
| Frequency noise and offset | B | 0.02 | 0.10 |
| Leakage resistance | B | 0.30 | 0.65 |
| Detector gain error and linearity | B | | 0.47 |
| Total (RSS) | B | 0.30 | 0.81 |

**Table 4.** Estimated Type B standard uncertainty components of automatic measurements.

The result using the automatic measurements made on March 21, 2009 expressed as the relative difference between the values that would be attributed to the nominal 10 V Josephson array standard by NIST ($U_{NIST}$) and its theoretical value ($U_{BIPM}$) is:

$$(U_{NIST} - U_{BIPM}) / U_{BIPM} = - 7.0 \times 10^{-11} \quad \text{and} \quad u_c / U_{BIPM} = 1.1 \times 10^{-10}$$

where $u_c$ is the combined standard uncertainty.

## 6. Discussion and conclusion

The preliminary measurements demonstrated NIST's ability to perform accurate and precise automatic 10 V measurements.

During the subsequent five days, experiments were carried out on various parts of the whole system (assemblage of the BIPM standard and the NIST measurement set-up) in order to identify sources of noise, to determine some critical parameters and to correct for their influences on the measurements.

In particular, we have confirmed that the EIP counters (that of the BIPM and those operated in the NIST laboratory) at the frequencies of these experiments perform within the measurement uncertainty claimed by the manufacturer [7] (Cf. Appendix A – 21 March 2009).

Concerning the evaluation of the leakage resistance, three different methods (Cf. Appendix A) were used to measure the leakage resistance between the measurement leads. The results are consistent and allow us to state that the contribution coming from the insulation resistance is a function of the arrangement of the comparison setup and may vary according to the comparison scheme, mostly because of different possible paths to ground. It is recommended that the leakage resistance be determined at the time of each comparison exercise.

This comparison allowed both the BIPM and the NIST to characterise more accurately and improve the robustness of their equipment and measurement setups.

During the period dedicated to the comparison, we were able to carry out the two options of the BIPM.EM-K10b comparisons. The results are shown in Fig. 9.
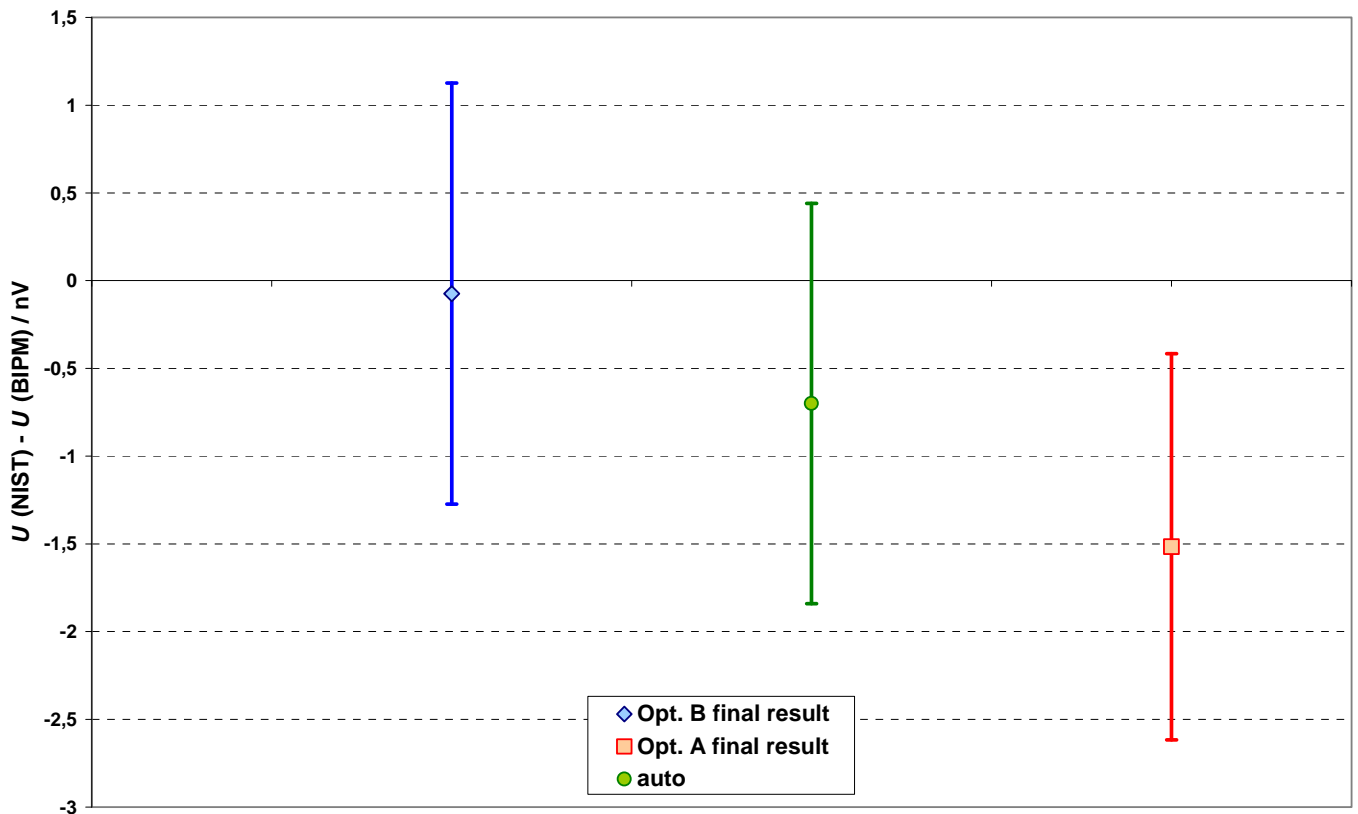
**Fig.** 10. Comparison results obtained from the 3 different measurements methods: options A & B of BIPM.EM-K10.b and NIST automatic measurements (uncertainty bars are $k$=1).

The final result of the option A measurements is a consequence of the weight of the first series of the measurement carried out on the 23rd of March, where the mean of 11 points show a voltage difference of -3 nV with a standard deviation of the mean of 0.85 nV. The use of an analog detector (option A) rather than a digital nanovoltmeter is known to lead to more sensitive measurement conditions.

We thus suspect a systematic error in the first series of 11 points of the option A comparison. This error might come from an error in the calibration of the BIPM measurement chain but we think that it has another source. The 2nd run of option A had measurements of 11 points. The mean difference was 0.03 nV with a standard deviation of the mean of 1.08 nV. The mean difference of the two runs of option A is 1.53 nV with a standard deviation of the mean of 0.75 nV.

There were two main changes between the two option A runs:

1 - Replacement of the BIPM RF sources: the Gunn-diode operated during the first series of measurement showed an abnormal behaviour. A loss in the frequency stability could lead to a systematic error or significant increase of noise (and this is not the case).

2- The CJVS DC bias source was kept on during the second run, i.e. the low side of the NIST array was kept connected to the potential of the virtual ground of the source.

During the comparison, the Helium Dewars of both JVS systems were closed in such a way that the regulation of the internal pressure was done by a pressure relief valve. The valve releases the excess gas every time the pressure reaches a certain level. The depression causes a temperature drop in the Dewar that can lead to a modification of the thermal EMFs. This phenomenon might explain the variation in the thermal EMFs observed during the comparison (Cf. Fig. 5). Further investigation of this particular topic is required.

The final result of the comparison is considered as the average value of the BIPM.EM-K10.b option A and option B results and is equal to:

$(U_{NIST} - U_{BIPM}) / U_{BIPM}$ = -8 × 10$^{-11}$ and $u_c / U_{BIPM}$ = 9.5 × 10$^{-11}$

Note: The uncertainty was calculated as followed:

The pooled Type A uncertainty is 0.53 nV, the quadratic combination of the Type A uncertainties of the two different options:

Opt A: $u_A$ = 0.75 nV

Opt B: $u_B$ = 0.75 nV (1/f noise floor of the NIST CJVS null detector)

As the two JVS involved in the comparison are the same in the two options, there is a strong correlation (but not total) between the results that have to be taken into account for the computation of the uncertainty of the final result.

For this, one has to consider in each uncertainty budget the part of the Type B uncertainties that are correlated and the one that are not:

$$u^2_{op.A} = u^2(correlated) + u^2_{op\_A} (uncorrelated)$$

$$u^2_{op.B} = u^2(correlated) + u^2_{op\_B} (uncorrelated)$$

The pooled Type B uncertainty of the final result (mean value of the two results) is then:

$$u^2 = u^2\text{(correlated)} + [u^2{}_{\text{op\_A}} \text{ (uncorrelated)} + u^2{}_{\text{op\_B}} \text{ (uncorrelated)}]/4$$

The details of the Type B uncertainty components (taken from tables 1 to 3) are given in the following table:

|  |  | BIPM contribution/ nV | NIST contribution/ nV |
|---|---|---|---|
| Components Correlated | Frequency stability | 0.02 | 0.10 |
|  | Leakage Resistance of the Meas. Leads | 0.30 | 0.65 |
| Components uncorrelated | Detector | 0.25 | 0.58 |

The final combined standard uncertainty is equal to 0.95 nV, calculated as the RSS of the pooled Type A uncertainty and pooled Type B uncertainty.

We reevaluate the uncertainty using 0.68 nV, the standard deviation of the mean of 37 points as the Type A uncertainty in the NIST measurements (Option B). The combined standard uncertainty $u_c$ is equal to 0.94 nV using the same method described above. This is because the conventional calculation for Type A uncertainty is close enough to the 1/f noise floor and does not have much impact to the final combined uncertainty.

**The authors are indebted to Tom Witt for his noise analysis on the series of measurements performed automatically.**

# References

[1] **Witt T.J.,** *Pressure Coefficients of Some Zener Diode-Based Electronic Voltage Standards*, IEEE Trans. Instrum. Meas. Vol.48 (2), pp. 329-332, April 1999.

[2] **Djordjevic S., Solve S.,** et al., *Direct comparison between a programmable and a conventional Josephson voltage standard at the level of 10 V*, Metrologia, 2008, 45(4), 429-435.

[3] **Hamilton C. A., Tang Y. H.**, *Evaluating the uncertainty of Josephson Voltage Standards,* Metrologia, 1999- **36**, pp. 53-58.

[4] **Y.Tang , M.A.Lombardi, and D.A.Howe**, "Frequency Uncertainty Analysis for Josephson Voltage Standard," Digest of Conf. on Precision Electromagnetic Measurements (CPEM2004), June 28- July 2, 2004, London, United Kingdom, pp. 338-339 (June, 2004).

[5] **Y.Tang, B. Wood and C. Hamilton,** *A Two-way Josephson Voltage Standard Comparison between NISN and NRC*, IEEE Trans. Instrum. Meas. Vol.58, pp. 821-826, April 2009.

[6] **Witt T.J.,** *Using the Allan Variance and Power Spectral Density to Characterize DC Nanovoltmeters*, IEEE Trans. Instrum. Meas. Vol.50 (2), pp. 445-448, April 2001.

[7] Field Note 5, Rev 02/90, EIP Microwave Inc.

[8] **S. Solve, R. Chayramy, S. Djorjevic and O. Séron**, *Comparison of the Josephson voltage standards of the LNE and the BIPM (part of the ongoing BIPM key comparison BIPM.EM-K10.b)* Metrologia Tech. Suppl*. **46** 01002, 2009.

**Appendix A**

This appendix describes the comparison measurements in a chronological manner.

**20 March 2009**

After having assembled the BIPM equipment, we cooled down the BIPM array (Hypres S/N 2538F-3) and varied the RF frequencies attainable with the sources (72 GHz to 78 GHz) to find adequate stable conditions for the voltage provided by the array. We didn't manage to get the appropriate stability and decided to replace the BIPM array with a backup one (Hypres S/N 2548E-6).

The critical current of this chip showed abnormally low value compared to the expected value (50 µA instead of 90 µA). After several thermal cycles, a suitable critical current of 80 µA was obtained.

Note: The BIPM JVS is not known to easily trap magnetic flux in its routine cooling conditions. One explanation for the trapping flux situation at NIST could be due to electrostatic effect following from the low level of relative humidity in the air (below 35 %).

The JVS systems were grounded to two different virtual grounds during the voltage adjustments of the arrays, but were floating from these grounds once the adjustments made. The shielding of the measurements leads and equipment were grounded to the earth ground of the laboratory.

The positive poles of the two quantum standards were connected together and the detector was inserted between the negative poles, with the high side of the detector connected to the BIPM JVS side. The JVS were directly connected in such a way that each polarity reversal of the standards had to be done at the same time. Even if this operation was performed in a reasonably short amount of time, the nanovoltmeter sometimes transmitted intially an "overload" error message on the IEEE bus, probably because of a transient.  However, the DVM returned to its correct operational status after a few seconds.

The first series of preliminary measurements gave a voltage difference between the two systems of +1.5 nV with a standard deviation of 3.1 nV.

A fit was applied to the data by the software and all the results were presented in a report following this computation policy. However, we used a traditional and simplified method to calculate the results from the raw data.  The results showed no large discrepancies.

At the end of the day, an automatic comparison following the NIST protocol was run that lasted all night. Unfortunately, the measurements stopped after 48 points because of instability of the RF power of the BIPM frequency source.

**21 March 2009**

We started the day by checking the accuracy of the frequency of the RF sources with a traditional experiment where an additional frequency mixer is added to the RF source setup (Gunn source+isolator+mixer) in order to measure the locked frequency with another EIP578B counter.

The experiment was carried out in as follows:

- The locked frequency of the NIST RF source was measured by the BIPM EIP 578 counter and gave the following result: $f_{NIST}$ = (75.833 700 000 + 0.000 000 007) GHz

- The locked frequency of the BIPM RF source was measured by a NIST EIP 578B counter  and gave the following result: $f_{BIPM}$ = (75.594 000 000 + 0.000 000 005) GHz

The results of this experiment show that the BIPM and NIST EIP counters measure a frequency in the GHz range within the uncertainties claimed by the manufacturer [6].

1- Relatively stable conditions were found on the BIPM system when biasing it at one of the two possible NIST CJVS operating frequencies ($f$ = 76.84 GHz) and 5 consecutive points were measured.

2- 5 points were measured in the configuration where the detector is reversed, i.e. the High of the nanovoltmeter to the NIST side.

3- 3 points were measured using the conditions described in (1) then a relative instability on the BIPM array led us to use a more stable one (Cf. point 4).

4- The BIPM RF source was set to $f$ = 76.850 GHz and 2 more points were measured.

5- Both JVS were switched to a frequency of $f$ = 76.76 GHz. The High of the DVM was moved back to the BIPM side and 5 points were measured.

6- 10 consecutive points were measured using the opposite configuration of the detector (i.e. High of the nanovoltmeter to the NIST CJVS side);

7- 5 more points were made using the configuration described in (5).

No significant discrepancies resulting from the DVM reversal were found.

The BIPM JVS was biased at $f$ = 76.765 GHz and some measurements were run automatically (NIST protocol) overnight and the next day.

**23 March 2009**

The BIPM measurement chain was installed in order to carry out an option A comparison.

While satisfactory stability was found on the positive polarities of both JVS, the NIST CJVS was significantly unstable on the negative polarity. This effect was worse when the BIPM JVS DC source was on.

The reason was probably due to the leakage currents that were found on the NIST CJVS: the Helium dewar was driven to two different potentials: one imposed by the 10 MHz reference potential and the other one from the virtual ground of the DC biasing source. The shielding of the biasing cable was disconnected on one side and the shielding of the complete measurement loop was rearranged in order to limit the leakage current.

We also found out that both instrument racks were not powered from the same mains source and we corrected this.

The BIPM array was biased at $f$ = 76.764 880 GHz in order to get a voltage difference between the two JVS that was compatible with the 3 µV range of the analog detector. In this configuration, the theoretical voltage difference is ($U_{NIST} - U_{BIPM}$) = 0.76658 µV and 11 consecutive points were successfully recorded.

**24 March 2009**


**Option B: replacement of the BIPM RF source**
We moved back to the option B comparison scheme where the BIPM and NIST arrays were biased at $f$= 76.764 880 GHz and $f$= 76.76 GHz respectively. We managed to measure only one point because the frequency of the BIPM RF source showed an abnormal behaviour that was identified as a periodic interruption of the signal. A failure in the BIPM RF source was suspected. We replaced the source and the BIPM array was then biased at $f$ = 74.549 570 GHz. The DVM that monitors the voltage across the BIPM array was removed and 6 points were measured.


**Measurements at the zero volt level**
At this point, we decided to carry out some measurements at the 0 V level (i.e. the arrays were biased on their zero volt step or close to it). Twenty successive points were obtained automatically during lunch time and the results are presented in **Fig.** A1. The results show an average value of ($U_{NIST} - U_{BIPM}$) = 0.55 × 10$^{-9}$ V with a standard deviation of the mean of $\sigma_A$ = 0.65 × 10$^{-9}$ V

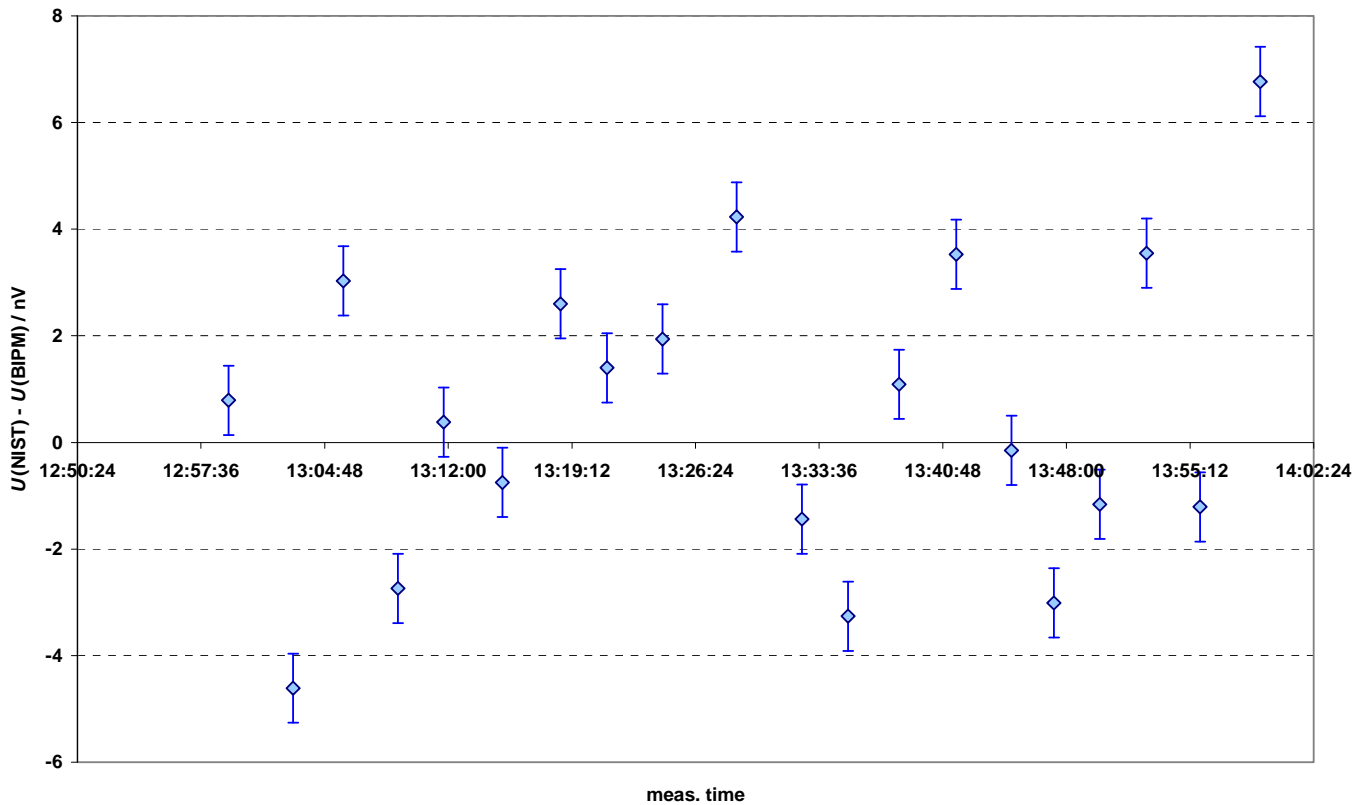**Fig.** A1. Voltage difference $U$(NIST) - $U$(BIPM) at the zero voltage level of the JVS.

This result is comparable to the one obtained at the 10 V level and indicates that the voltage drop induced by the leakage is insignificant. In other words, this experiment leads us to conclude that there is no systematic leakage error at the 10 V level. The Type A uncertainty which is of the order of 0.7 nV reflects the noise level that is induced in the measurement loop. This noise level does not seem to depend on the voltage level.

**Measurement leads resistance and insulation resistance**

During the afternoon, we ran a series of leakage current measurements in order to estimate the uncertainty related.

The leakage resistance, $R_i$, of the filter capacitances between the measurement leads resistance, $r_B$, is responsible for a voltage drop error in the voltage generated by the JVS. To calculate the uncertainty component due to these leakage currents, both resistances have to be measured. First, to estimate the resistance of the voltage output leads, we carried out a measurement with the cryoprobe leads connected to the array at 4 K (measurement leads, biasing leads , voltage leads) according to the schematic shown in **Fig.** A2.
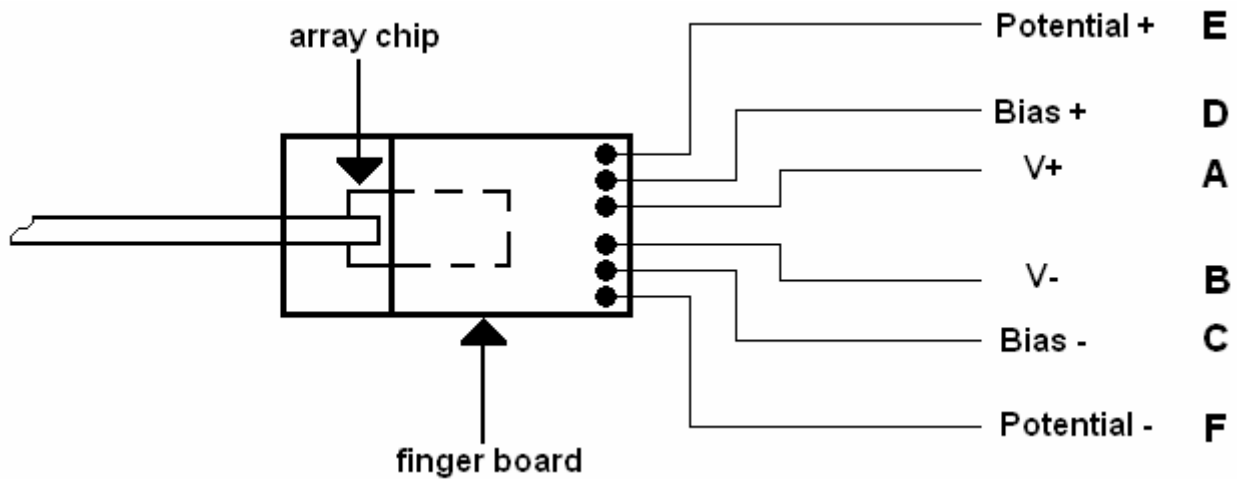
**Fig.** A2. Details on the connection of the leads (potential, bias and measurement) on the finger board.

The measurements are presented in the following table (Cf. **Table** A1):

| Resistance Meas. | NIST CJVS ($\Omega$) | BIPM JVS ($\Omega$) |
|---|---|---|
| AE; BF | 5.6; 4.4 | 2.8; 2.7 |
| DE; FC | 5.6; 5.4 | 2.9; 2.9 |
| AD; CB | 5.5; 4.0 | 2.0; 2.0 |
| ADE*; BFC* | 8.3; 6.9 | 7.7; 7.6 |

**Table** A1. Results of the measurements of the resistance of the biasing and measurement leads while connected to the array at 4 K.

* Those components represent the sum of the resistance of the three leads (i.e. terminals ADE and BCF are shorted).

Note: a residual resistance of 0.1 ohm (multimeter offset error) was subtracted from all the measurements.

The resistance value of each individual lead can then be calculated from the formulas:

$$D = ADE - AE; A = ADE - DE; E = ADE - AD;$$
$$F = BCF - BC; B = BCF - FC; C = BCF - BF;$$

And the resistance of the measurement leads is deduced from the formula: $r_B = E + F$;

$r_B$ (NIST) = 5.75 $\Omega$

$r_B$ (BIPM) = 2.95 $\Omega$

Second, the leakage resistance of each JVS was determined from three experiments:

**Leakage resistance measurement (NIST methodology)**

A measure of the leakage resistance between the ground and each measurement lead of both JVS is performed following the NIST methodology depicted in Figure A3. The measurement can be done with the array immersed in liquid helium.
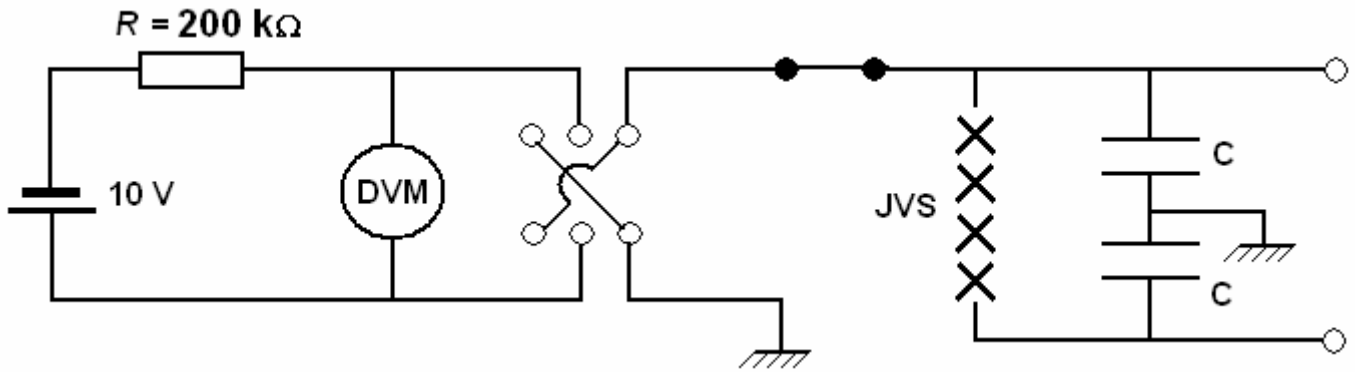


**Fig.** A3.  Schematic of the experiment setup to measure the leakage resistance between each measurement lead and the ground.

To estimate the leakage, we first disconnected the battery from the probe. The DVM then recorded the battery voltage as a base line. Then the battery was connected to one of the precision leads and the ground. The voltage drop after the capacitor was fully charged is associated with the leakage resistance. The third step was to reverse the battery polarity to check the symmetry of the leakage resistance. Finally, the battery was disconnected from the probe to ensure there was no drift in the voltage during the measurement.  The measurement generally produced a leakage current that was about 4 times greater than the direct leakage measurement between the two precision leads because the capacitor leakage paths were effectively in parallel rather than in series. Thus the leakage resistance was calculated using the formula $R_i = 4U / i_F$ where $U$ is the voltage of the source and $i_F$ is the leakage current. The DVM measured the time dependence of the voltage across a 200 k$\Omega$ resistor ($R$) that connected one side of the array to the ground. The other side, at a potential of 10 V, was left open so that the only path to ground was through $R_i/2$. The bias source was disconnected, leaving $R_i$ as only the isolation resistance of the cryoprobe. These measurements were carried out successively in both polarities. For example, Figure A4 and A5 represent the records obtained from the measurements performed on the BIPM probe (negative polarity) and NIST probe, respectively.
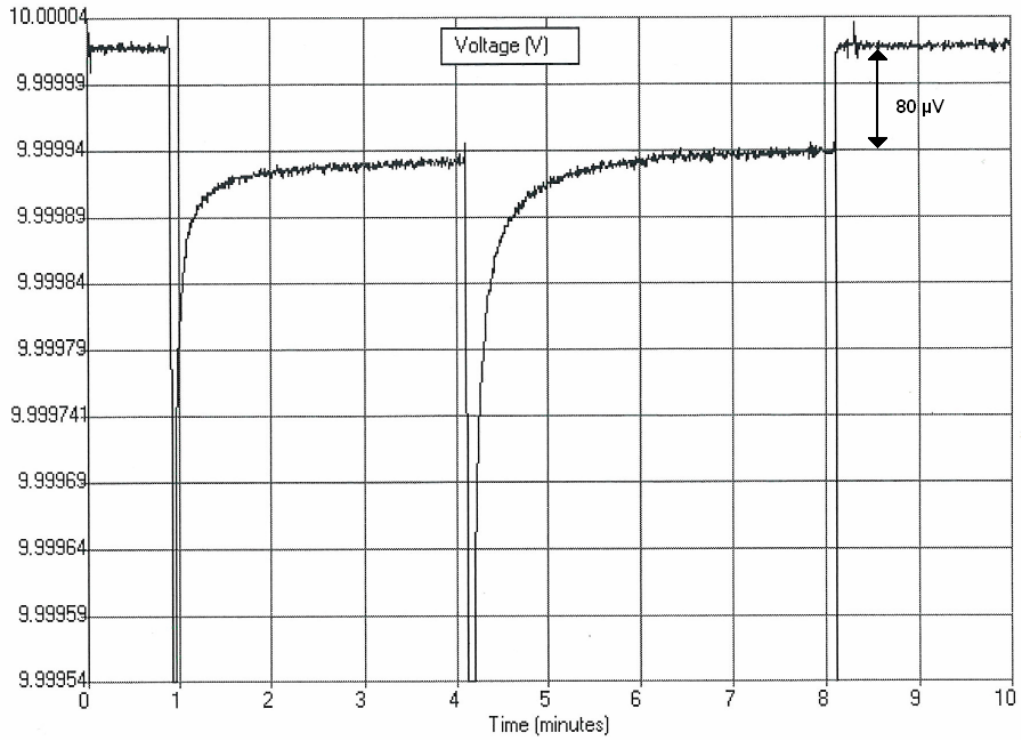
**Fig.** A4.  Charge and discharge through the filter capacitors between a precision lead and ground on the BIPM probe.
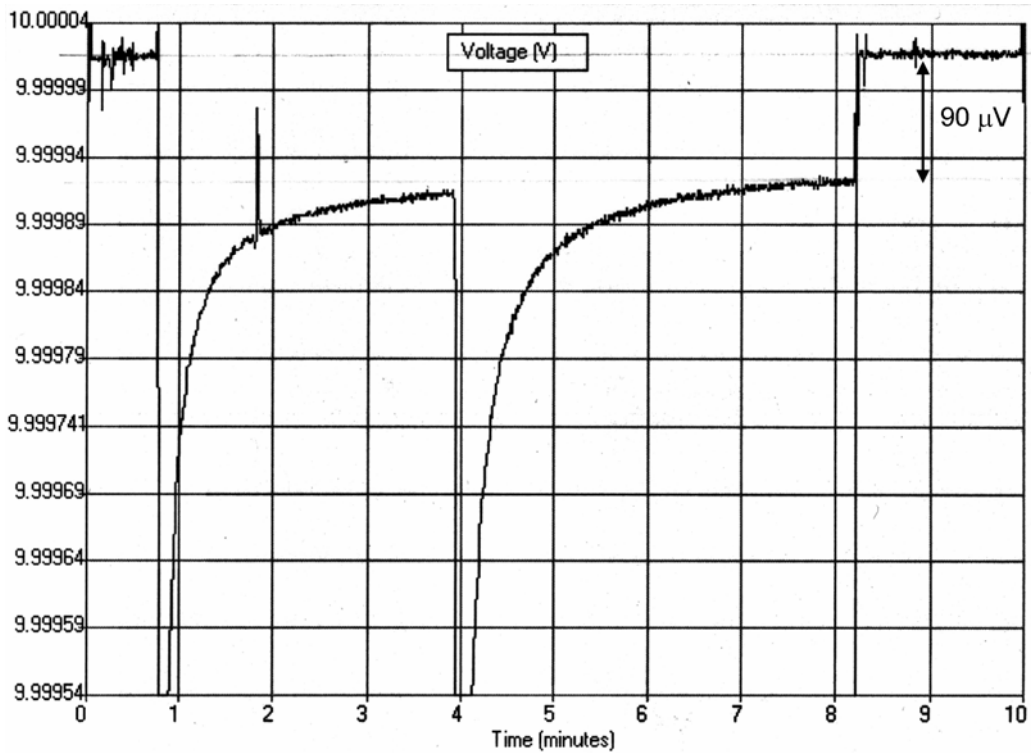


**Fig.** A5.  Charge and discharge through the filter capacitors between a precision lead and ground on the NIST probe.

At 240 s after the polarity reversal, the leakage current has reached the asymptotic value corresponding to the long-term value of the apparent insulation resistance. Within this assumption, the remaining voltage difference between both polarities ($\Delta e$) allows for the calculation of the leakage current ($i_F$) according to the formula: $i_F = \Delta e/2R$ and $R_i = 4U / i_F$. The uncertainty due to the leakage resistance can thus be determined (Cf. Table A2).

| | CJVS | BIPM |
|---|---|---|
| Leads resistance $r_B$ ($\Omega$) | 5.75 | 2.95 |
| Leakage current $i_F$ (pA) | 450 | 400 |
| Leakage resistance $R_i$ ($\Omega$) | $8.9 \times 10^{10}$ | $1.0 \times 10^{11}$ |
| Uncertainty (V) $\dfrac{r_B}{R_i} \times U$ | $6.5 \times 10^{-10}$ | $3.0 \times 10^{-10}$ |

Table A2. Uncertainty due to the leakage currents for both Josephson systems at the nominal voltage $U$ of 10 V.

**Leakage resistance measurement (BIPM methodology)**

A complete description of this method is given in [8]. Unfortunately, we were not able to carry out this experiment on the CJVS because its biasing current source is referenced to a virtual ground. However, the experiment was performed on the BIPM JVS and gave the following result:

$R_i = 1.1 \times 10^{11}$ ohms, which is in good agreement with the value of $R_i$ given in **Table** A2.

**Leakage resistance measurement (direct measurement)**

A third method consisting of a direct measurement of the leakage was performed with a Keithley 500 Megaohmmeter. Once both JVS were warmed up, and the arrays removed from their respective cryoprobes, a direct measurement of the insulation resistance between the measurement leads was carried out and the results are presented in **Table** A3.

| | CJVS | BIPM |
|---|---|---|
| $R_i$ ($\Omega$) | 1 to $2 \times 10^{11}$ | 2.5 to $5 \times 10^{11}$ |

Table A3. Insulation resistance between the two measurement leads of the JVS. (Evolution from 1 to 5 minutes).

From these measurements, we can conclude that all of the leakage determination results are consistent. The first two methods (NIST and BIPM methodologies) are more accurate than a direct measurement. However, the direct measurement method gives a quick order of magnitude of the true value.

**Option A comparison: second run**

The end of this day was dedicated to a second run of the Option A scheme where the BIPM array was biased at $f$ = 76.549 480 GHz. Eleven points were performed and the NIST CJVS biasing source was kept on during this measurement session, meaning that the low side of NIST array was connected to the potential of the virtual ground of its DC biasing source.